Article

Selective C–C and C–H Bond Activation/Cleavage of Pinene Derivatives: Synthesis of Enantiopure Cyclohexenone Scaffolds and Mechanistic Insights

Ahmad Masarwa, Manuel Weber, and Richmond Sarpong

J. Am. Chem. Soc., **Just Accepted Manuscript** • Publication Date (Web): 19 Apr 2015

Selective C–C and C–H Bond Activation/Cleavage of Pinene Derivatives: Synthesis of Enantiopure Cyclohexenone Scaffolds and Mechanistic Insights**

Ahmad Masarwa, Manuel Weber and Richmond Sarpong*

Department of Chemistry, University of California, Berkeley, CA 94720 (USA), E-mail: rsarpong@berkeley.edu

Keywords: C–C / C–H Activation/Cleavage • Rhodium Catalysis • Rearrangements • Pinene Derivatives • Natural Products

Abstract

The continued development of transition metal-mediated C–C bond activation/cleavage methods would provide even more opportunities to implement novel synthetic strategies. We have explored the Rh(I)-catalyzed C–C activation of cyclobutanols resident in hydroxylated derivatives of pinene, which proceed in a complementary manner to the C–C bond cleavage which we have observed with many traditional electrophilic reagents. Mechanistic and computational studies have provided insight into the role of C–H activation in the stereochemical outcome of the Rh-catalyzed C–C bond activation process. Using this new approach, functionalized cyclohexenones that form the cores of natural products including the spiroindicumides and phomactin A have been accessed.

Introduction

Carbon-hydrogen (C–H) and carbon-carbon (C–C) bonds are ubiquitous in organic molecules. As such, advances that accomplish the selective activation and functionalization of C–H and C–C bonds have the potential to revolutionize the synthesis of complex organic molecules. While methods for C–H activation/functionalization[1] have grown exponentially over the last decade, comparatively few methods for C–C bond activation have emerged.[2] General and effective methods for C–C activation are likely to change the practice of complex molecule chemical synthesis just as C–H activation/functionalization logic is beginning to influence the synthesis of complex molecules.[3] In particular, methods to selectively activate a desired C(sp^3)–C(sp^3) bond using transition metal complexes remains difficult to achieve.[2] In order to make C–C bond activation processes broadly applicable in complex molecule synthesis, their scope and limitations need to be identified. This can be effectively achieved by exploring these methods in functional group rich, complex settings such as those encountered in natural product scaffolds. In this Article, we report our studies in this direction, which has focused on C–C bond activation/cleavage reactions of cyclobutanols, accessed in two steps from carvone, to yield functionalized cyclohexenone derivatives (e.g., **2** and **3,** Figure 1) that comprise the cores of several natural products. We also provide mechanistic insights into these Rh(I)-catalyzed transformations.

As a part of a general program to synthesize natural products including suaveolindol (**4**, Figure 1), phomactin A (**5**), spiroindicumides A and B (**6** and **7**), and others (**8**–**11**), we recognized that the core scaffold of these compounds could arise from sustainable, readily available, and inexpensive carvone. A key challenge in achieving a unified strategy to these compounds (in particular **4**–**7**) would rely on identifying a divergent reaction on each enantiomer of carvone that would lead to the programmed installation of the C4 all-carbon quaternary stereocenter present in **2**, ***ent*-2**, **3** and ***ent*-3** (see box in Figure 1).

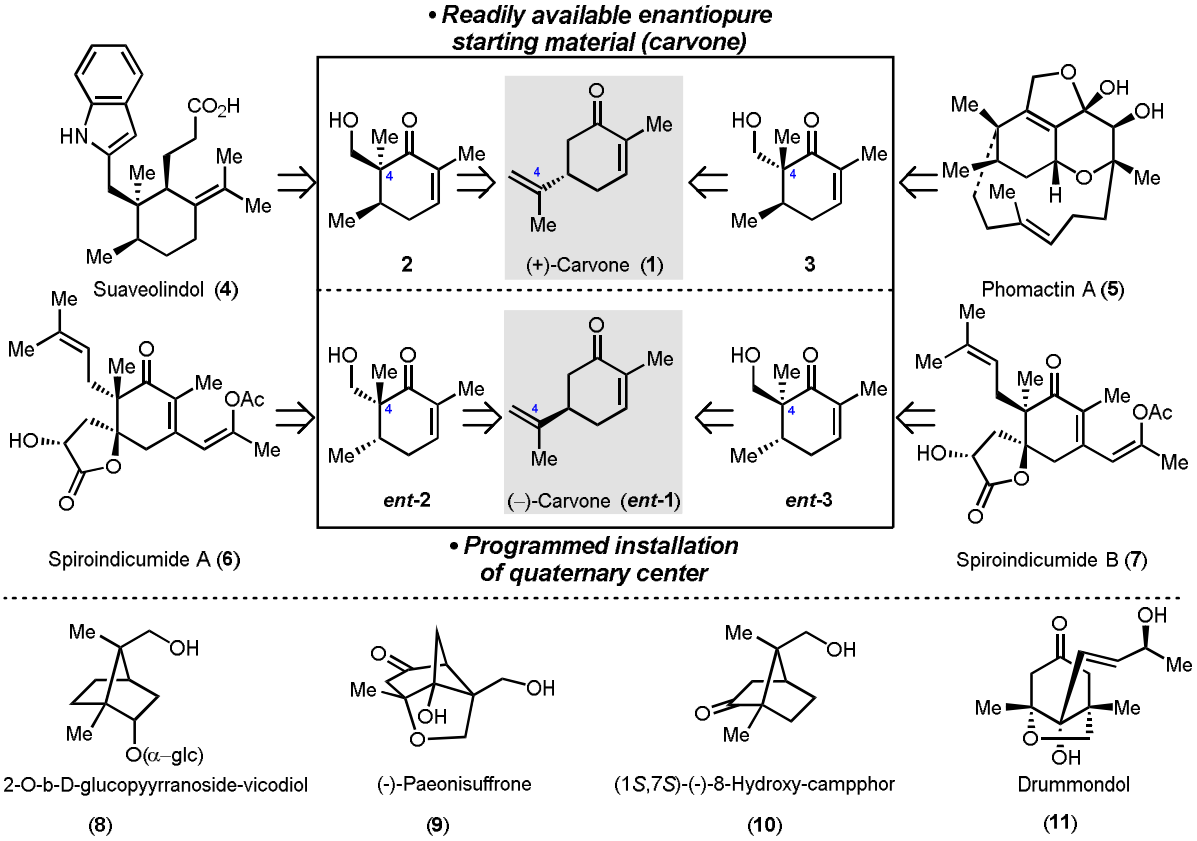

Figure 1. Unified, carvone-based, strategy to natural product core scaffolds.

Results and Discussion

We commenced our studies with the conversion of (+)-carvone (**1**) to a diastereomeric mixture of epoxides (**12**; 1:1 d.r.) upon treatment with *m*-CPBA. Subjecting the diastereomers of **12** to *in-situ* generated bis(cyclopentadienyl) titanium chloride (Cp_2TiCl) yields readily-separable cyclobutanol-containing bicycles **13a** and **13b** (ratio of 3:2), following the precedent of Bermejo and coworkers.[4] We have obtained unambiguous support for the structures of **13a** and **13b** using X-ray crystallographic analysis (see CYLviews in Scheme 1).[5] This is a readily scalable route and multigram quantities of **13a/b** can be accessed in a single pass.

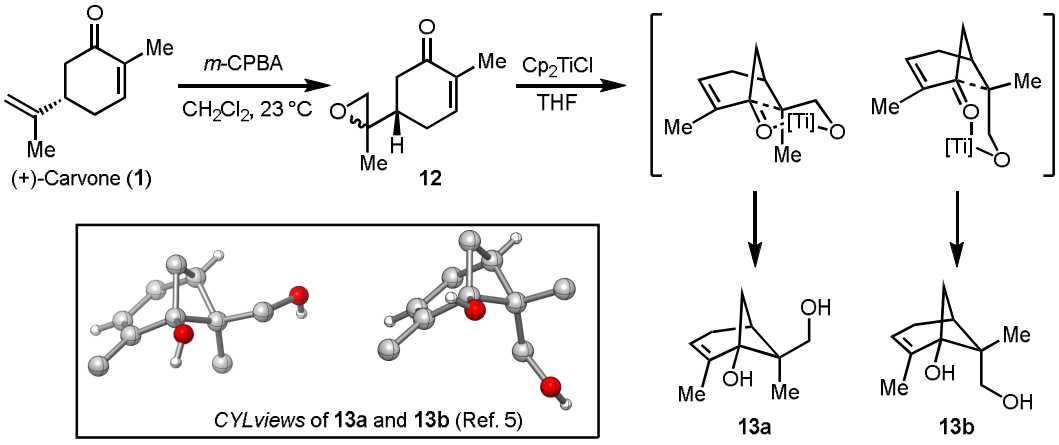

Scheme 1. Synthesis of cyclobutanol diastereomers **13a** and **13b**.

We envisioned that diastereomers **13** would serve as substrates in C–C bond activation and cleavage processes to yield substituted cyclohexenones such as **2** and **3** as well as the cores of **8**–**11**. As illustrated in Figure 2, complementary fragmentation scenarios could be imagined (e.g., for **13a**). While opening of the cyclobutane ring was anticipated on the basis of strain release considerations,[6] it was unclear which C–C bond would be cleaved (C1–C2 vs. C1–C4). It was our expectation that through the appropriate choice of activating agent (transition metal complex or traditional electrophiles/oxidants), selectivity for the cleavage of either C–C bond could be achieved.

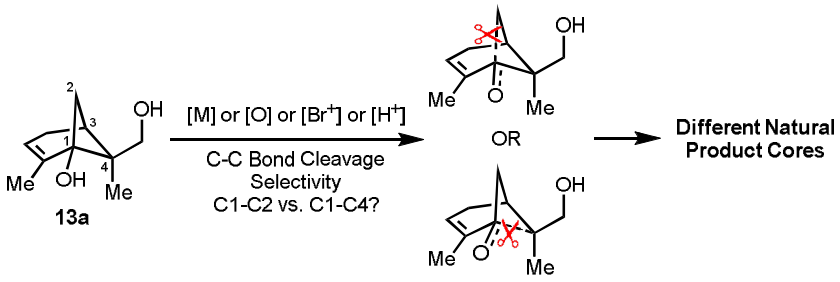

Figure 2. Proposed tactics for selective C-C bond cleavage in pinene derivatives, exemplified for **13a**.

Despite the existing wealth of information on the skeletal rearrangement/fragmentation of pinene and associated derivatives,[7] the rearrangement chemistry of hydroxylated variants such as **13a** and **13b** have not been investigated. Thus, we initiated our studies on the C–C bond activation/cleavage of **13a/b** using well-established reagents for the fragmentation/ rearrangement of pinene (e.g., *m*-CPBA). Treatment of **13a** with *m*-CPBA (Scheme 2A) leads to a diastereoselective epoxidation of the pinene derivative, which is then transformed to **15** (confirmed by X-ray crystallographic analysis) in 78% yield *via* **14**. Similarly, **13b** (Scheme 2B) rearranges to **17** and **18** (both confirmed by X-ray analysis) upon treatment with *m*-CPBA in 93% combined yield. Compound **17** (which maps on to the core of the natural product **8**)[8] arises from migration of the most substituted proximal C1–C4 bond (grey arrow in **16**), whereas bridging tricycle **18** (the core of the natural product **9**)[9] results from opening of the epoxide intermediate (blue arrow in **16**) by the pendant primary hydroxy group.

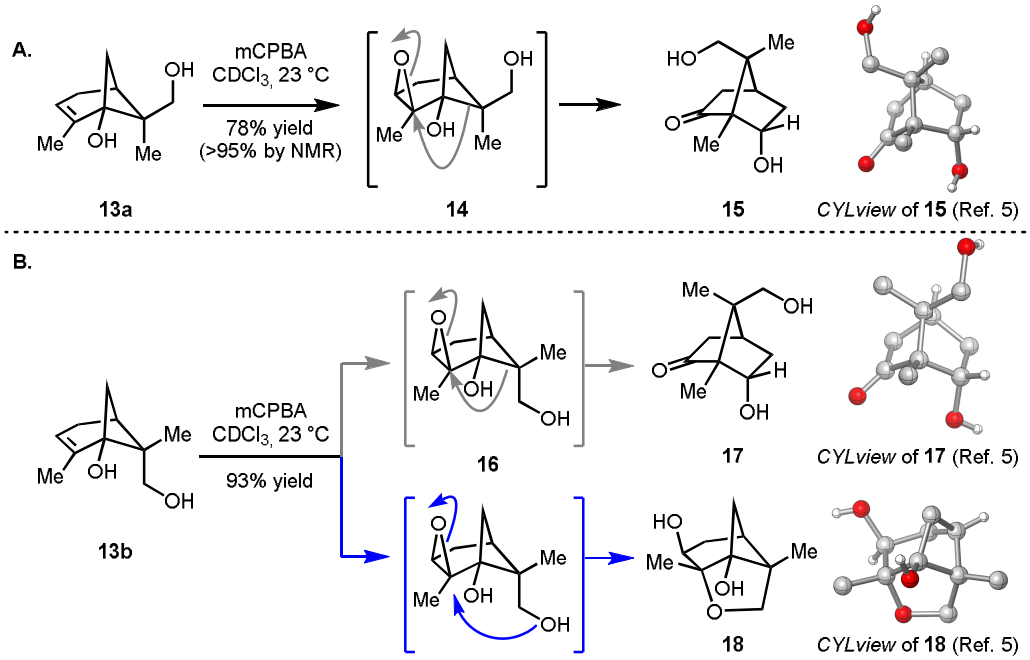

Scheme 2: *m*-CPBA-Promoted selective C1–C4 bond cleavage/ rearrangement of **13a** and **13b**. B: When $CDCl_3$ was used as the reaction solvent, a 1:9 ratio of **17**:**18** was observed, whereas in CH_2Cl_2 a 1:3 mixture was formed.

In addition, when **13a** was subjected to a BrØnsted acid (PPTS) (Scheme 3A), the intermediate tertiary carbocation (**19**) rearranges to **20** as a result of the cleavage/migration of the more substituted C1–C4 bond. In the same fashion, **13b** was transformed to naturally occurring **10**[10] and **21** (Scheme 3B), where the incipient carbocation is intramolecularly intercepted by the primary hydroxy group.[11]

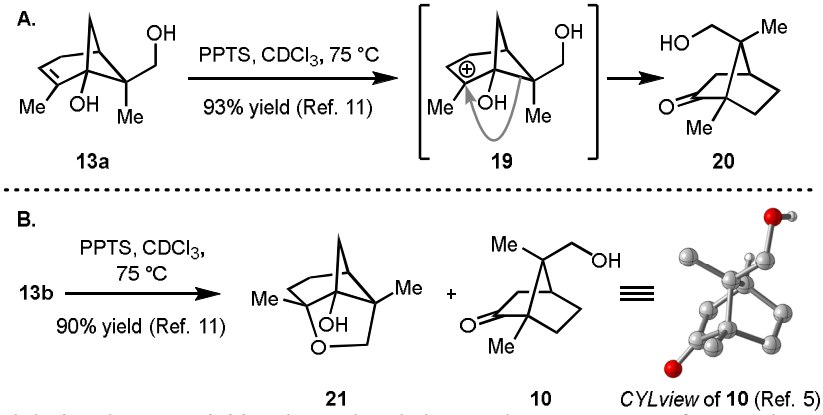

Scheme 3: Products formed during the PPTS-initiated C–C bond cleavage/rearrangement of **13a** and **13b**.[11] Products **21** and **10** were formed in a 1:0.2 ratio alongside with a C1-C2 cleavage/rearrangement product.

Treatment of **13b** with *N*-bromosuccinimide yields **25** (Scheme 4A), where a bridging ether linkage has formed *via* the intermediacy of **23** and **24**, whereas exposure of diastereomer **13a** to the same conditions gives a lactone **28** *via* **26** and **27** (Scheme 4B).[12]

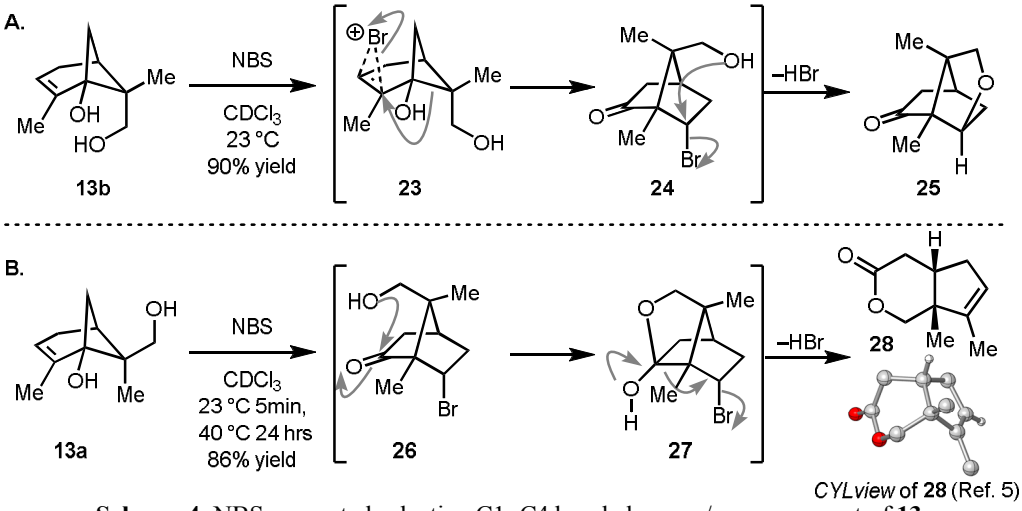

Scheme 4. NBS-promoted selective C1–C4 bond cleavage/rearrangement of **13**.

All the rearrangements of the pinene derivatives described thus far have involved the cleavage of the more substituted C1–C4 bond. In molecules such as **13**, the C1–C4 bond is the weaker, longer bond (compare X-ray bond length in **13a**: C1–C2 = 1.551 Å, C1–C4 = 1.567 Å; **13b**: C1–C2 = 1.535 Å, C1–C4 = 1.589). In addition, the cleavage of the C1-C4 bond favors the antiperiplanar relationship with either the epoxide (in **14** and **16**; Scheme 2A and 2B) or the bromonium moiety (in **23**; Scheme 4A and 4B). These observations are consittent with previous observations for pinene derivatives.[7c] In order to access natural product cores such as **2** and **3**, the less substituted, proximal, C1–C2 bond has to be cleaved. To achieve this goal, we sought to employ transition metal complexes. It is well established that transition metal complexes can be sterically and electronically tuned (by the choice of metal or ligand) to exhibit a preference for the carbon (1°, 2° or 3°) on which the metal would reside on an incipient organometallic intermediate (e.g., primary C(sp3)-[M] species vs. a tertiary C(sp3)-[M]). This outcome can either be thermodynamic (if the process is reversible) or kinetic (i.e., reflected in the transition state energies).[2,13] Over the last decade, significant advances have been made in the use of transition metal complexes to facilitate the opening of strained cyclic compounds.[13] Of the complexes that have been reported to effect these transformations, Rh complexes have emerged as the most generally applicable.[14]

We initiated our Rh-catalyzed ring opening investigations using conditions developed by Murakami[15] and by Cramer[16] with **13a**/**b** as the substrates (Scheme 5). Cyclohexenones **2** and **3** as well as **29** and **31** and phenol side product **30** were obtained following complete consumption of the starting material under the stated conditions. All of the observed products result from selective C1–C2 bond cleavage (C1–C4 ring opening products have not been observed). Following optimization, conditions to selectively access **2**, **29**, **3** as well as **30**[17] were identified.[18] For diastereomer **13a**, the addition of *S*-BINAP as a ligand to the standard conditions was beneficial[19] and resulted in the formation of **29** as the exclusive diastereomer[20] (with respect to the C5 stereocenter, Scheme 5). The formation of **2** as the major product could be achieved only when $[Rh(COD)OH]_2$ was used as the catalyst at low temperature (see entry 3).[21] At the lower temperature (i.e., 40 °C) phenol **30** was only observed in trace amounts, since the retro-aldol step that is required for its formation (see below) may require a higher temperature to proceed. A longer reaction time (Scheme 5, entry 3: 48 h *vs*. entry 1: 1.5 h) allowed us to isomerize **29** to the thermodynamically favored conjugated enone **2** (compare also Scheme 5

bottom: isomerization of **31** to **3**). However, with diastereomer **13b** as the substrate, the standard conditions with a catalytic amount of $[Rh(COD)OH]_2$ in the absence of *S*-BINAP proved superior, giving **3** in high yield.[22]

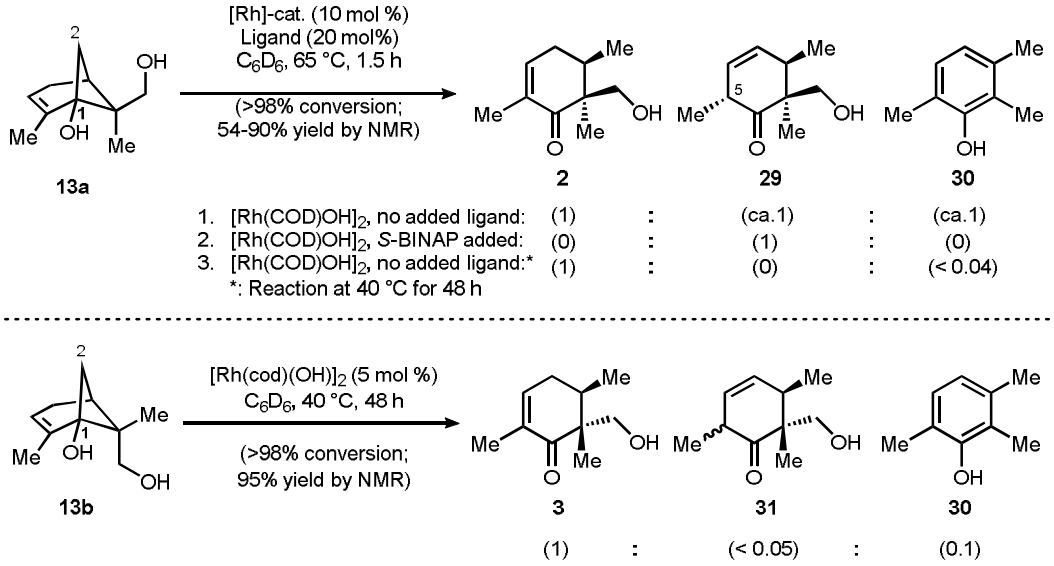

Scheme 5. Selective Rh-catalyzed C1–C2 bond cleavage/rearrangement of **13**.

Mechanistically, products **2** and **3** could arise from a simple protonolysis of the alkyl-Rh intermediate **2-Rh** (Scheme 6B). However, a rationale for the formation of **29**, **31**, and **30** required further insight into the mechanism of the C–C bond cleavage process. To this end, exposure of **13a-Ac** (Scheme 6C), bearing an acetyl group on the primary hydroxyl, to the reaction conditions led to clean conversion, suggesting that deprotonation of the primary hydroxyl in **13a** is not a requirement for the Rh-catalyzed cyclobutanol opening. In contrast, bis-acetyl substrate **13a-Ac$_2$** did not react, which supports the importance of deprotonation involving the tertiary hydroxy group of **13a** to the cyclobutane opening step.[23] We have also conducted deuteration studies to gain more insight into the fate of the initially formed organo-Rh intermediate (i.e., **2-Rh**). Using diastereomer **13a-D$_2$** (Scheme 6A) in the presence of D_2O, with $[Rh(COD)OH]_2$ as catalyst and *S*-BINAP as a ligand, we observed 98% D incorporation in **29-D** at C5 and none at C2, indicating that the newly introduced hydrogen at C2 is likely delivered intramolecularly. This newly introduced proton at C2 could either result from a 1,3-Rh shift[24] (Scheme 6B, Path A) or through a series of isomerization reactions (occurring by β-H elimination and re-addition of [Rh-H];[25] Scheme 6B, Path B). In Path A (i.e., after alkoxy-Rh **13a-Rh** undergoes selective C1–C2 bond activation to give alkyl-Rh complex **2-Rh**), an ensuing 1,3-Rh shift would yield π-allyl-Rh intermediate **29a-Rh** *via* **2'-Rh**. Metal enolate **29a-Rh**, may be protonated or deuterated to give **29a-E** as a single diastereomer. This diastereoselectivity could arise from the fact that the primary OH/OD group triggers the protonation/deuteration, since a mixture of diastereomers (**29a-E**) is observed for the protonation of **29a-Rh** where R = Ac. However, this position (i.e., C5) is fairly acidic and epimerization was observed when the reaction was allowed to proceed over longer periods, and during silica gel chromatographic purification. However, in the crude reaction mixture, only a single diastereomer was observed i.e., **29a-E** (where E, R = H, D). Alternatively, in Path B, alkyl-Rh intermediate **2-Rh** or the allylic Rh species (**2'-Rh**) may undergo β-H-elimination followed by isomerization to give **32/33,** which converts to **30** by retro-aldol reaction.

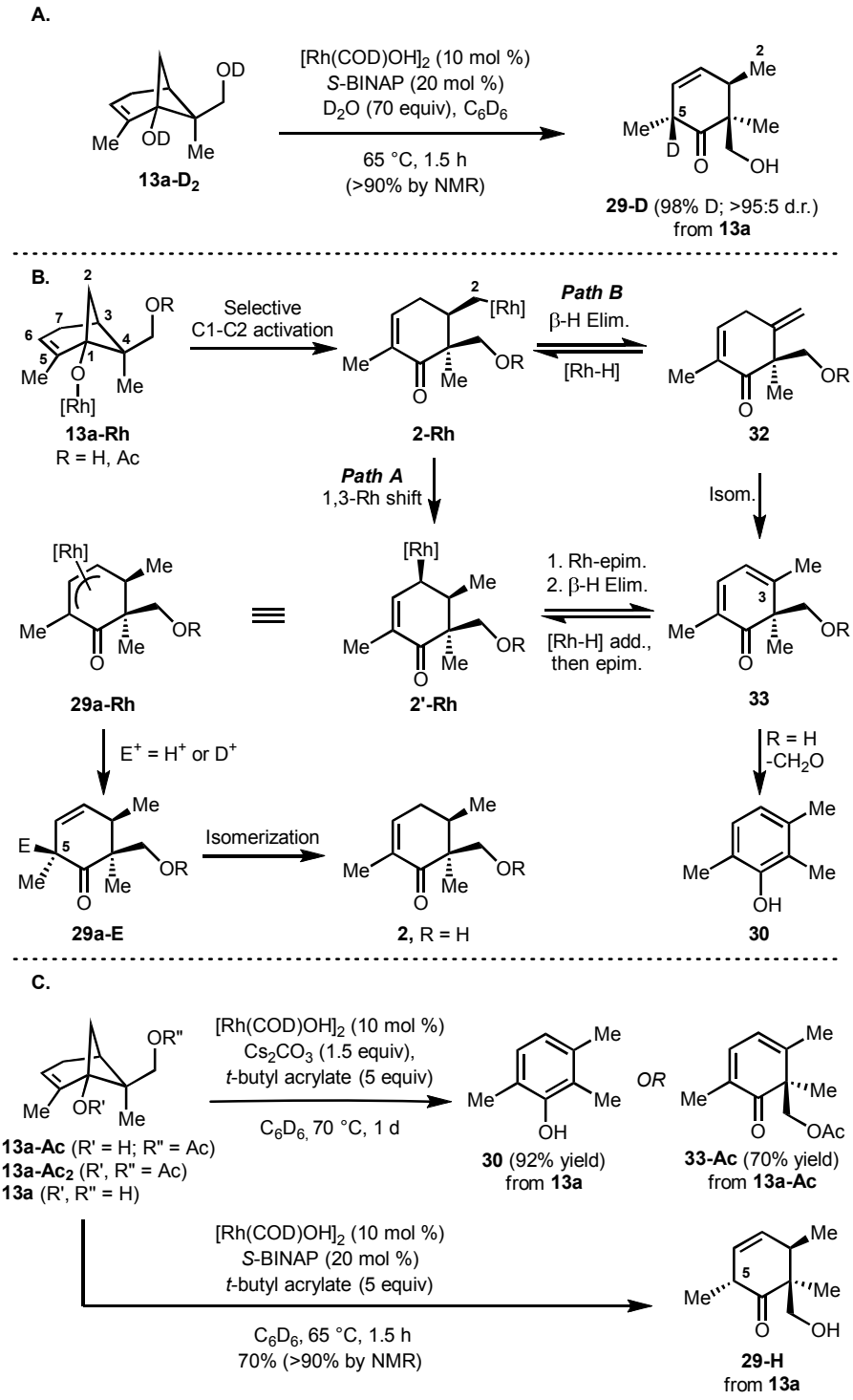

Scheme 6. A: Deuteration studies; B: Mechanistic hypothesis of the Rh(I)-mediated transformations; C: Reactions with *t*-butyl acrylate as an additive. (add. = addition, elim.=elimination, epim.=epimerization)

In an attempt to intercept the presumed [Rh-H] species that may be generated from **2-Rh**, we added *t*-butyl acrylate as a [Rh-H]-acceptor (Scheme 6C). In the presence of *t*-butyl acrylate (5 equiv), **13a** is converted to phenol **30** under the stated conditions. However, **13a-Ac**, bearing an acetyl group, is selectively converted to **33-Ac** under the same conditions, supporting the intermediacy of dienone **33**[26] (where R = H, Scheme 6B) in the formation of phenol **30**.[27] Changing the ligand from COD to *S*-BINAP resulted in a substantial increase in the

selectivity of the product formation (compare entries 1 to 2 in Scheme 5). An even more significant difference was observed when *t*-butyl acrylate was added to the reaction mixture; with COD as ligand, phenol **30** was obtained as the sole product (see Scheme 6C). On the other hand, using *S*-BINAP as the ligand (under otherwise identical conditions, Scheme 6C), **29-H** was formed as the major product, without any trace of **30** observed. It therefore appears that when using *S*-BINAP as the ligand, a direct 1,3-Rh shift (Path A, Scheme 6B) is dominant over Path B. However, the mechanism of the 1,3-Rh migration[16] remained to be fully elucidated.

On the basis of our combined observations, a 1,3-Rh migration would most likely occur through C–H activation involving **2-Rh**.[28] In the expected C–H activation process, the Rh migrates from a thermodynamically less favored alkyl C(sp^3) to a more favored allylic C(sp^3) position, (see **2-Rh→2'-Rh/29a-Rh**, Scheme 6). The likelihood of such an allylic C(sp^3)–H activation step is in agreement with the recent elegant observations of Lam and coworkers.[29] In their studies, the unexpected migration of Rh from a thermodynamically more favored vinyl C(sp^2) to a less favored allylic C(sp^3) position *via* C–H activation was observed.

To support the proposed C–H activation in the 1,3-Rh migration, we have undertaken computational analysis of the overall process (**A** → **F**) as summarized in Figure 3.[30]

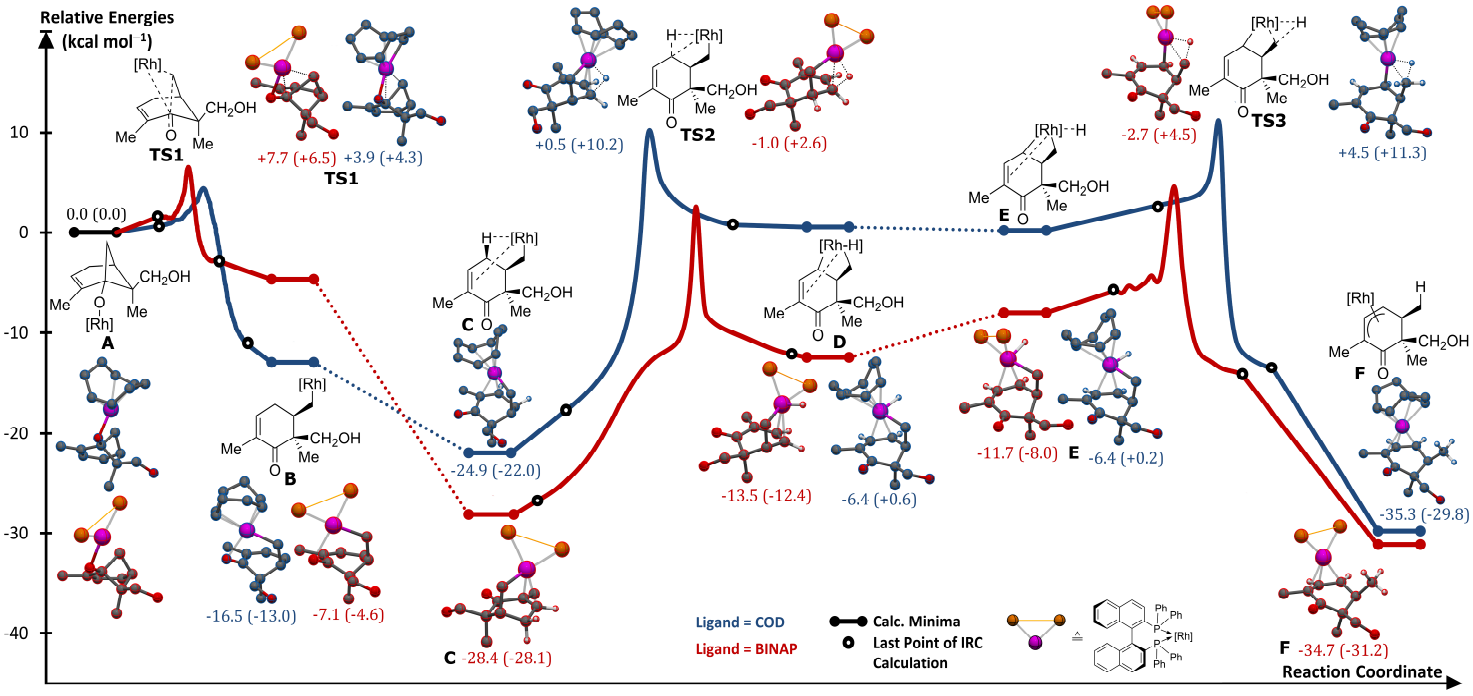

Figure 3. Energy profile of the CC-/CH-activation and reductive elimination steps for the transformation of **13a-Rh** → **2'-Rh**. Numbers represent relative energies reported in kcal mol^{-1} at the DFT/M06-L/6-311+G(d,p)/LanL2DZ-F level in benzene and include zero-point energy correction. Numbers in brackets are gas-phase energies from IRC calculation and do not include zero-point energy correction.

We found that the C–C bond activations (**A** → **TS1** → **B**) with either COD (blue lines) or *S*-BINAP (red lines) as ligands, show reasonable activation barriers of 3.9 and 7.7 kcal mol^{-1}, respectively. However, the most important difference was found in the stereospecific 1,3-Rh migration step by an oxidative C–H insertion and ensuing reductive elimination process (**C** → **F** *via* transition states **TS2** and **TS3**). A total energy demand of 27.4 kcal mol^{-1} was found when *S*-BINAP was modeled as the ligand, and 29.4 kcal mol^{-1} for COD. In general, these barriers indicate the feasibility of such a 1,3-Rh-migration through C–H activation. Although the barrier

for the C–H activation (**C** → **D**) is lower when COD is modeled as the ligand ($\Delta\Delta G^0$ = 2.0 kcal $^{-1}$), the reductive elimination (**E** → **F**) was calculated to be lower by 3.7 kcal mol^{-1} for the *S*-BINAP ligand. The lower overall barrier of the Rh-shift process for the *S*-BINAP system ($\Delta\Delta G^0$ = 2.0 kcal $^{-1}$) may indicate that with this ligand, a C–H activation scenario is kinetically more favored than in the case with COD as the ligand.

Experimentally, such a C(sp^3)–H bond activation is supported by several observations. First, tricycle **21** (Scheme 7A) is converted to **3** upon exposure to a catalytic amount of the Rh-precatalyst and *R*-BINAP.

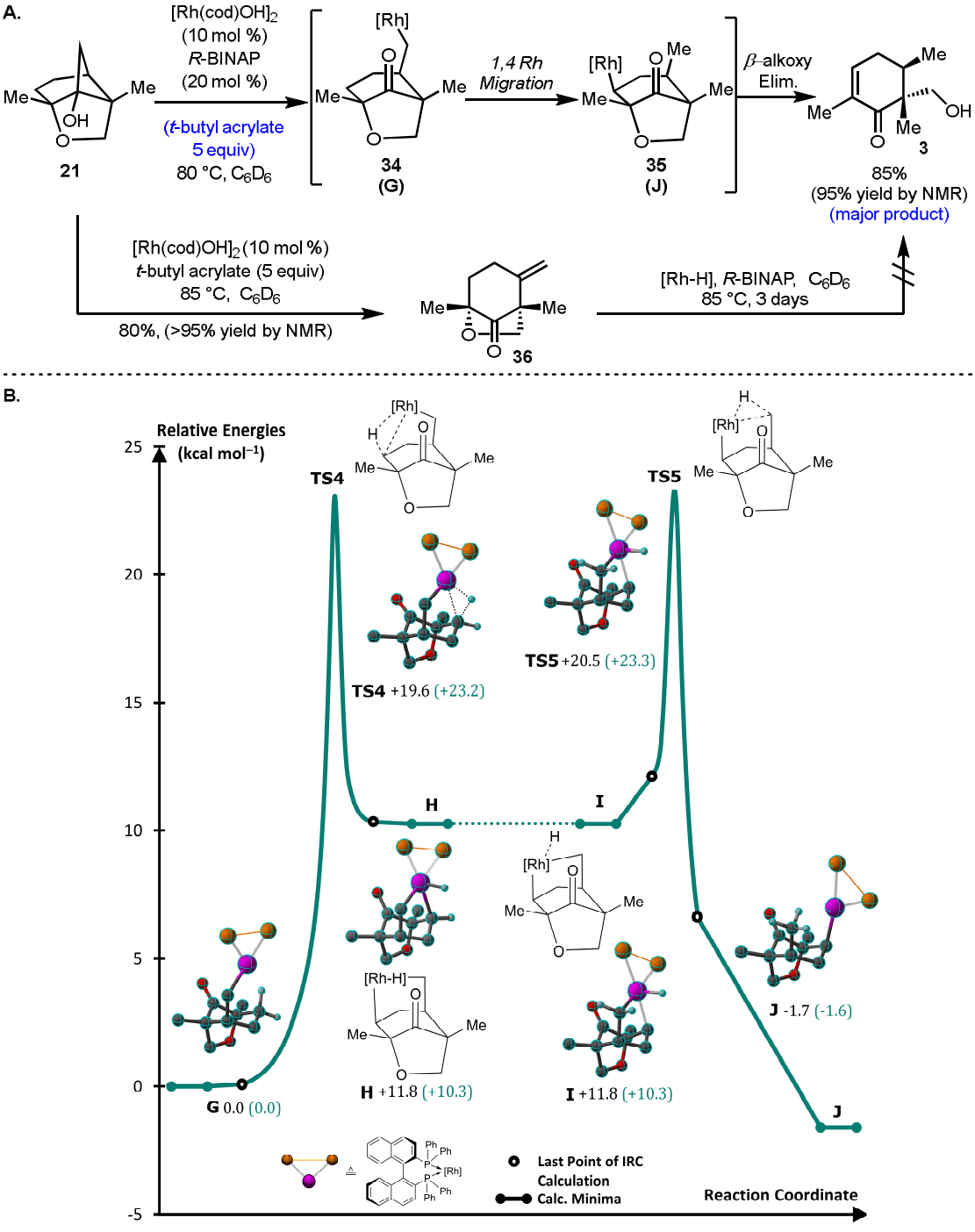

Scheme 7. A: Selective Rh-catalyzed C-C/C-H activation for **21** and stereospecific synthesis of **36**. B: Energy profile of the stereospecific 1,4-[Rh] shift **G** → **J**. Numbers represent relative energies reported in kcal mol^{-1} at the DFT/M06-L/6-311+G(d,p)/LanL2DZ-F level in benzene and include zero-point energy correction. Numbers in brackets are gas-phase energies from IRC calculation and do not include zero-point energy correction.

We believe this transformation proceeds *via* **34**, which following a net 1,4-Rh migration by C–H activation affords **35** that undergoes β-alkoxy elimination to give **3**. Of note, when **21** is subjected to the standard conditions (i.e., in the absence of *R*-BINAP, see Scheme 7A), the addition of *t*-butyl acrylate as a hydride acceptor leads to the exclusive formation of **36**,[31] while in the presence of *R*-BINAP (blue highlighting in Scheme 7A), **3** is formed as the major product. These observations suggest that with BINAP as ligand, a stereospecific Rh-shift is dominant, whereas with COD as the ligand, β-H elimination becomes significant, leading to a complex reaction mixture, presumably proceeding through an isomerization process.

For the transformation of **21** to **3**, the isomerization pathway[25] is very unlikely, since the re-addition of [Rh-H], bearing the bulky *R*-BINAP ligand, would have to occur from the sterically less accessible α-face (i.e., concave face) of **36** in order to give **3** where both vicinal Me-groups are syn disposed.

The unlikelihood of a Rh-H isomerization pathway is further supported by the observation that in the reaction of cyclohexanone **36** with *in-situ* generated [Rh–H], **3** is not observed as a product.[32] The activation barrier for a stereospecific 1,4-Rh migration[28] proceeding by C(sp^3)–H activation was computed at 19.6 kcal mol^{-1} (see Scheme 7B) and the barrier for the subsequent reductive elimination was computed as 8.7 kcal mol^{-1}, which are in agreement with reported systems.[30]

Conclusion

In summary, a series of enantiopure cyclohexenone and cyclohexanone derivatives (e.g., **2**, **3**, **17**, and **36**) that comprise the cores of several natural products (**4**, **5**, **8**, and **11**, respectively) have been accessed from readily available carvone. Key to these transformations is a selective C–C bond activation/cleavage. Traditional electrophilic reagents as well as Rh(I) complexes were employed in order to achieve complementary C–C bond cleavages. Our mechanistic investigations into the Rh-catalyzed C–C activation indicate that a subsequent Rh migration most likely proceeds by C–H activation. To the best of our knowledge, this work represents the first observations of a 1,3- and 1,4- C(sp^3) to C(sp^3) Rh migration occurring through C–H bond activation.[33]

Supporting Information Available

Experimental and computational details, analytical and supplemental data for the prepared compounds can be found in the electronic supporting information. . This information is available free of charge via the internet at http://pubs.acs.org.

Acknowledgments

The authors thank the Rothschild Foundation and VATAT (The Israeli Council for Higher Education) for postdoctoral fellowships to A.M. and the DAAD (German Academic Exchange Service) for a postdoctoral fellowship to M.W. We thank Dr. A. DiPasquale for solving the crystal structures, supported by NIH Shared Instrument Grant (S10-RR027172) as well as NSF CHE-0840505 for funding computational resources at UCB

and Dr. Kathleen Durkin for assistance. Funding was in part provided by the NSF under CCI center for selective C-H functionalization (CHE-1205646)

References and Notes

[1] For reviews see: a) Ackermann, L. *Acc. Chem. Res.* **2014**, *46*, 281; b) Engle, K. M.; Mei, T.-S.; Wasa, M.; Yu, J.-Q. *Acc. Chem. Res.* **2012**, *45*, 788; c) Ackermann, L.; Modern Arylation Methods, Wiley-VCH, Weinheim, **2009**; d) Bergman, R.G. *Science* **1984**, *223*, 902.

[2] a) Murakami, M.; Ito, Y. in *Topics in Organometallic Chemistry*. Vol. 3, Springer, Berlin **1999**, pp 97; b) Jun, C. H. *Chem. Soc. Rev.* **2004**, *33*, 610; c) Rybtchinski, B.; Milstein, D. *Angew. Chem. Int. Ed.* **1999**, *38*, 870; d) Marek, I.; Masarwa, A.; Delaye, P.-O.; Leibeling, M. *Angew. Chem. Int. Ed.* **2015**, 54, 414; e) Dong, G. (Ed.), *Top. Curr. Chem.* "C−C Bond activation" Vol 346, Springer, Berlin **2014**; f) Ruhland, K. *Eur. J. Org. Chem.* **2012**, 2683; g) Aïssa, C. *Synthesis* **2011**, 3389; h) Murakami, M.; Matsuda, T. *Chem. Commun.* **2011**, *47*, 1100; i) Park, Y.J.; Park, J.-W.; Junn, C.-H. *Acc. Chem. Res.* **2008**, *41*, 222; j) Murakami, M.; Makino, M.; Ashida, S.; Matsuda, T. *Bull. Chem. Soc. Jpn.* **2006**, *79*, 1315; k) Tunge, J. A.; Burger, E. C. *Eur. J. Org. Chem.* **2005**, 1715; l) Jun, C.-H. *Chem. Soc. Rev.* **2004**, *33*, 610; m) Perthuisot, C.; Edelbach, B. L.; Zubris, D. L.; Simhai, N.; Iverson, C. N.; Müller, C.; Satoh, T.; Jones, W. D. *J. Mol. Catal. A* **2002**, *189*, 157.

[3] For a recent example, see: Yamaguchi, J.; Yamaguchi, A. D.; Itami, K. *Angew. Chem. Int. Ed.* **2012**, *51*, 8960.

[4] Bermejo, F. A.; Mateos, A. F.; Escribano, A. M.; Lago, R. M.; Burón, L. M.; López, M. R.; González, R. R. *Tetrahedron* **2006**, *62*, 8933–8942.

[5] X-Ray structures were visualized with CYLview, 1.0b; Legault, C. Y., Université de Sherbrooke, **2009** (http://www.cylview.org). Most of the hydrogen atoms are removed for clarity.

[6] Cyclobutanes have an inherent ringstrain of 28 kcal/mol, see ref 13a.

[7] a) Erman, M.B.; Kane, B. J. *Chem. Biodivers.* **2008**, *5*, 910; b) Mann, J.; Davidson, R. S.; Hobbs, J. B.; Banthorpe, D. V.; Harborne, J. B. Natural Products, Addison Wesley Longman Ltd. Harlow, UK, **1994**, pp 309; c) Bhattacharyya, P. K; Prema, B. R.; Kulkarni, B. D.; Pradhan, S. K. *Nature* **1960**, *187*, 689.

[8] Gan, L.-S.; Zhan, Z.-J.; Yang, S.-P.; Yu; J.-M. *J. Asian Nat. Prod. Res.* **2006**, *8*, 589.

[9] a) Shibata, S.; Nakahara, M. *Chem. Pharm. Bull.* **1963**, *11*, 372; b) Aimi, N.; Inaba, M.; Watanabe, M.; Shibata, S. *Tetrahedron* **1969**, *25*, 1825; c) Yoshikawa, M.; Harada, E.; Kawaguchi, A.; Yamahara, J.; Murakami, N.; Kitagawa, I. *Chem. Pharm. Bull.* **1993**, *41*, 630; d) Martín-Rodríguez, M.; Galán-Fernández, R.; Marcos-Escribano, A.; Bermejo, F. A. *J. Org. Chem.* **2009**, *74*, 1798.

[10] This is the first non-biotransformation based preparation of **10**; for an earlier preparation see: Miyazawa, M.; Miyamoto, Y. *J. Mol. Catal. B.* **2004**, *27*, 83.

[11] See the supporting information for additional details and rearrangements where also a cleavage of the C1-C2 bond was observed.

[12] Treating **13a** with Br_2 instead of NBS also forms lactone **28** in similar yield.

[13] a) Seiser, T.; Saget, T.; Tran, D.N.; Cramer, N. *Angew. Chem. Int. Ed.* **2011**, *50*, 7740; b) Masarwa, A.; Marek, I. *Chem. Eur. J.* **2010**, *16*, 9712.

[14] a) Murakami, M. *Chem. Rec.*, **2010**, *10*, 326; b) Cramer, N.; Seiser, T. *Synlett* **2011**, 449.

[15] For a recent example, see: Yada, A.; Fujita, S.; Murakami, M. *J. Am. Chem. Soc.* **2014**, *136*, 7217.

[16] Seiser, T.; Cramer, N. *J. Am. Chem. Soc.* **2010**, *132*, 5340.

[17] See Scheme 6B for the selective synthesis of **30**.

[18] The relative configurations of **2** and **3** were elucidated by NOESY experiments and ^{13}C-NMR calculations, see supporting information.

[19] Using *R*-BINAP resulted in a "mismatch", impeding the ring opening reaction and giving a complex reaction mixture.

[20] The relative configuration of **29** was elucidated by NOESY NMR, see supporting information.

[21] Product **2** can also be obtained by a) treating **29** with a base (i.e. Cs_2CO_3, see supporting information) or b) under the $[Rh(COD)OH]_2$ conditions and a longer reaction time.

[22] For the most efficient access to **3**, see Scheme 7 top.

[23] The same results were obtained for the other diastereomer.

[24] For a 1,3-Rh shift by a proto-demetallation process see reference 16.

[25] Matsuda, T.; Shigeno, M.; Murakami, M. *J. Am. Chem. Soc*, **2007**, *129*, 12086.

[26] Importantly, dienone **33-Ac** could offer opportunities for oxygenation at C3 to access the spiroindicumides.

[27] Diastereomers **13b** and **13b-Ac** gave similar results, see supporting information for details.

[28] For examples of 1,4- and 1,5-Rh shifts from C(sp^3) to C(sp^2) by C-H activation, see: a) Seiser, T.; Roth, O. A.; Cramer, N. *Angew. Chem. Int. Ed.* **2009**, *48*, 6320; b) Ishida, N.; Shimamoto, Y.; Yano, T.; Murakami, M. *J. Am. Chem. Soc.*, **2013**, *135*, 19103.

[29] Burns, D. J.; Lam, H. W. *Angew. Chem., Int. Ed.* **2014**, *53*, 9931.

[30] This setup was recently used in many DFT investigations for Rh-catalyzed reactions, see: Yu, H.; Wang, C.; Yang, Y.; Dang, Z.-M. *Chem. Eur. J.* **2014**, *20*, 3839 and references therein. See the supporting information for further computational details.

[31] For a racemic access/isolation to such natural product (cores), see: a) Nagaraju, C.; Prasad, K. R. *Angew. Chem. Int. Ed.* **2014**, *53*, 10997; b) Shiao, H.-Y.; Hsieh, H.-P.; Liao, C.-C. *Org. Lett.* **2008**, *10*, 449; c) Milborrow, B. V. *Phytochemistry* **1975**, *14*, 1045; d) Powell, R. G.; Weisleder, D.; Smith, C. R. *J. Org. Chem.* **1986**, *51*, 1074.

[32] Although we observe slow conversion of **36** (ca. 45% after 1 day, ca. 70% after 3 days), only unidentified side products were formed. See the supporting information for details.

[33] CCDC 1051272 (**10**), CCDC 1051273 (**13a**), CCDC 1051274 (**13b**), CCDC 1051275 (**15**), CCDC 1051276 (**17**), CCDC 1051277 (**18**), CCDC 1051278 (**28**) contain the supplementary crystallographic data for this paper. These data can be obtained free of charge from The Cambridge Crystallographic Data Centre via www.ccdc.cam.ac.uk/ data_request/cif.

Table of Contents (TOC)

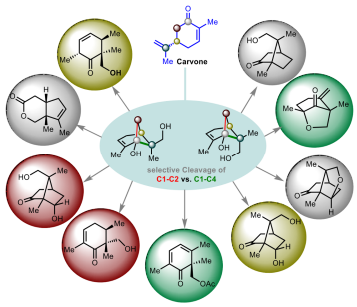

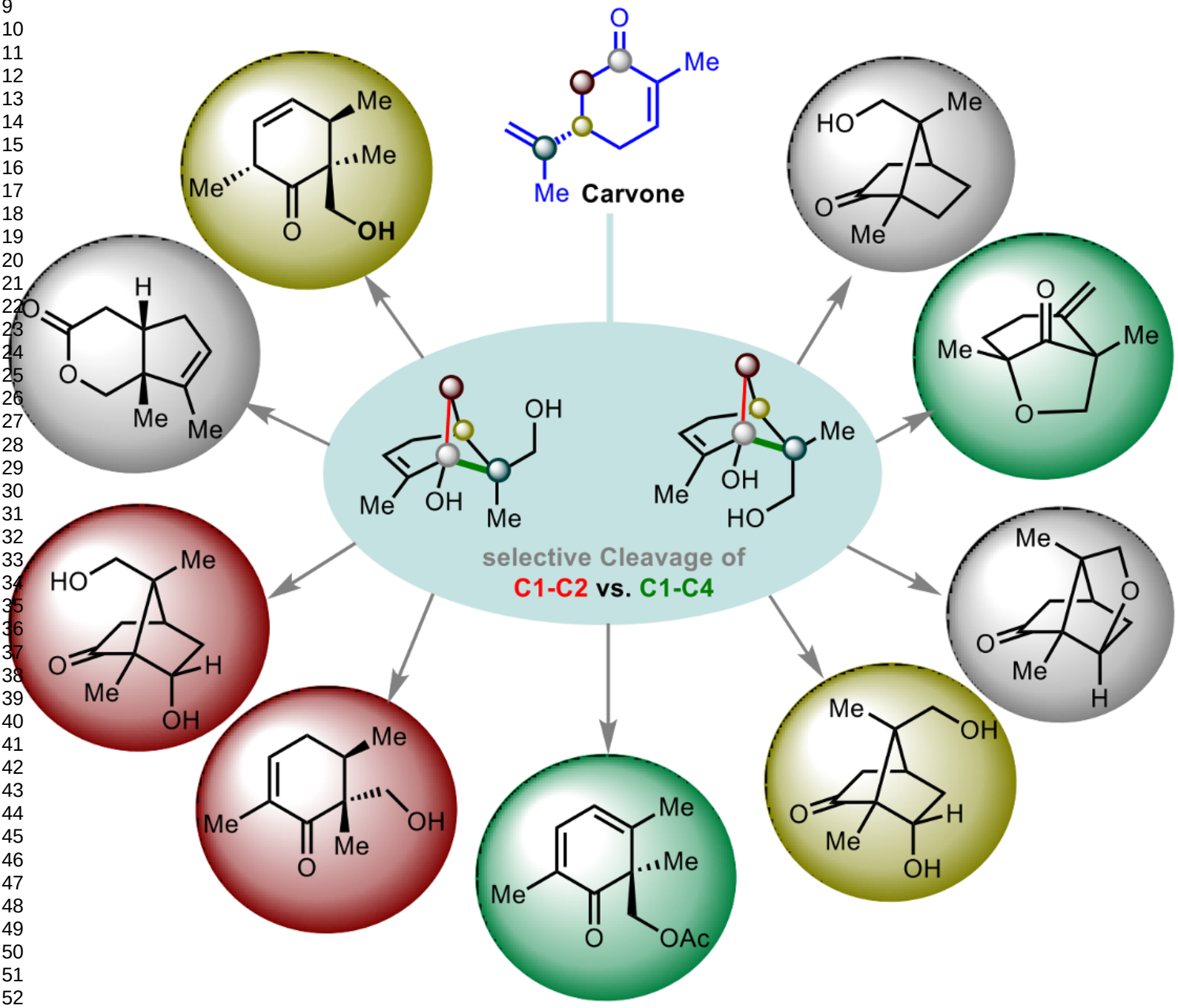
Carvone
selective Cleavage of
C1-C2 vs. C1-C4